International Journal of GEOMATE, June, 2024 Vol.26, Issue 118, pp.49-56
ISSN: 2186-2982 (P), 2186-2990 (O), Japan, DOI: https://doi.org/10.21660/2024.118.4354
Geotechnique, Construction Materials and Environment

NUMERICAL SIMULATION OF WAVE REDUCTION WITH MANGROVE FOREST USING DELFT3D MODELING AT BANYUGLUGUR BEACH

Retno Utami Agung Wiyono[1], Gusfan Halik*[1], Slamet Waluyo[1], and Risqi Sofiana[1]

[1]Civil Engineering Department, Jember University, Indonesia

*Corresponding Author, Received: 15 June 2023, Revised: 22 March 2024, Accepted: 25 March 2024

ABSTRACT: Coastal erosion caused by continuous sea wave action is destructive. One potential solution to reduce the impact of waves and coastal erosion is the utilization of mangrove forests as natural barriers. The Banyuglugur Coastal Area has a thriving mangrove forest that grows along 5.1 km of coastline. The objective of this research is to determine the percentage reduction of the mangrove forest as an energy buffer and the wave height along the Banyuglugur Coast. The method employed to achieve this goal involves numerical simulation using Delft3D, considering the influence of mangrove forest length, tides, wind, and wavelength. The Delft3D-Coupling model is used, combining two modules, FLOW for tidal simulation and WAVE for wind-wave simulation. Mangroves with a width of 70 m in Zone A are high-density mangrove locations that can reduce wave energy by 62.14%, while low-density mangroves in Zone D with a width of 30 m can reduce wave energy by 44.28%. The simulation results indicate that mangrove forests on Banyuglugur Beach, with an average width of 50 m, can dampen waves by an average of 52.8% and reduce the average wave height by 39% compared to incoming waves.

Keywords: Numerical Simulation, Wave Reduction, Mangrove, Delft3D, Banyuglugur Beach

1. INTRODUCTION

The coastline is a highly vulnerable area to ocean waves and coastal erosion. This phenomenon is of utmost concern in efforts to protect coastal environments and preserve their ecosystems. One potential solution to reduce the impact of waves and coastal erosion is the utilization of mangrove forests as natural barriers. The mangrove forests inhabiting the boundary between land and sea play a physical role in coastal areas, serving as protection against the impacts of storms, tsunamis, waves, and coastal erosion [1]. Coastal ecosystems like mangrove forests are often utilized as a tool in coastal defense, as the characteristics of mangrove trees can reduce wave height per unit distance, particularly in the physical presence of these mangrove trees [2].

Along with the increasing human population, mangrove forests are experiencing a decline in both their extent and quality. This decline is caused by the maximum utilization of mangrove forest natural resources, resulting in deforestation and degradation [3,4]. This phenomenon is experienced by Situbondo Regency, which has several mangrove forests in its coastal areas. The condition of mangrove forests in Situbondo Regency has experienced a significant decrease in area [5]. The main cause is the extensive logging of mangrove forests to clear land for ponds [6] and several areas prioritized as natural tourism destinations [7]. In recent years, efforts to improve land cover quality have been carried out by the Environmental Agency of Situbondo Regency in several coastal locations with mangrove forests [8], one of which is Banyuglugur Beach. This beach is one of the frequently visited tourist destinations and is a densely populated coastal area. In this regard, it is important to identify the ability of mangrove forests in their role as coastal protectors, especially to determine to what extent mangrove forests can reduce waves in the Banyuglugur Beach.

The attributes of ocean waves can be defined through wave measurements, physical models, numerical simulations, and analytical solutions [9]. The contribution of mangroves to hydrodynamic processes through numerical simulations is already well-known and thoroughly understood.

Numerous studies have been conducted to comprehend various aspects of mangroves, including root systems, trunks, their ability to reduce waves, and the deposition of fine sediments [2]. Some of them were using unstructured grid for wave reduction modeling, i.e. MIKE 21FM [10] and ADCIRC [11]. Other study utlizes Singapore Regional Modeling with combination in Delft3D modeling [12].

In term of Delft3D modeling for wave reduction due to mangrove, Tarya et al. [13] conducted numerical modeling employing a 40 m resolution rectangular grid to understand the impact of mangrove density on tidal dynamics in Segara Anakan Lagoon using Delft3D-Flow, while Xie et al. [14], using Delft3D to model the implications of coastal conditions and sea-level rise on mangrove

vulnerability with a rectangular grid resolution of 50 x 50 m.

Delft3D application is widely used in hydrodynamic modeling research due to its ability to conduct numerical modeling and provide various input parameters required for studies, offering a comprehensive simulation of coastal wave scenarios [15,16]. With the use of the same application, grid resolution and bathymetry determine the accuracy and efficiency of the results [17]. However, many grid cells with high grid resolution will require high computing time and power [18]. Therefore, proper grid resolution is necessary to obtain stable results and efficient computation time [19].

The previous studies on numerical simulation on waves reduction by mangrove utilized rectangular grid for simulation [13,14]. Meanwhile, curvilinear grid provides high resolution in coastal areas, especially in the examined regions, with resolution decreasing towards the sea. This study has a different approach by using curvilinear grid for wave simulation.

The advantage of the curvilinear grid is its ability to accurately represent complex boundaries and is produced quickly with higher quality [20]. This allows for efficiency in simulation time compared to rectangular grids with similar resolutions, which require longer simulation times. By using a curvilinear grid, the simulation results obtained will be more accurate because the high-resolution grid in the observed area can produce a more detailed and representative model.

Therefore, the aim of this research is to determine the percentage reduction of mangrove forests as energy buffers and wave attenuators along Banyuglugur Beach using Delft3D. By uncovering this aspect, the obtained information can support the improvement of coastal management strategies, enhance ecosystem-focused adaptation measures, and ultimately preserve the environmental sustainability and socio-economic well-being of coastal communities for the future.

In the next section, the research area and methodology will be presented. The research area includes the distribution of observation points, while the methodology involves the calculation of model input parameters and the simulation process. The simulation results will be presented and explained in detail, and visualized in the form of figures. Finally, conclusions regarding the reduction of waves by mangrove forests at the study site will be drawn.

2. RESEARCH SIGNIFICANCE

This simulation study focuses on the ability of mangrove forests to attenuate ocean waves. The research holds significant importance in providing an understanding of the extent to which mangroves can reduce wave intensity. Compared to another similar study, this study has a different approach by comparing five different mangrove widths. The information obtained can support the enhancement of coastal management strategies, enhance ecosystem-focused adaptation measures, foster the sustainability of coastal environments, and improve the socio-economic well-being of coastal communities for the future.

3. DATA AND RESEARCH METHODS

3.1 Research Sites

The research site at Banyuglugur Beach, Situbondo Regency, has thriving mangrove forests along the coastline, stretching approximately 5.1 km. These forests are divided into five zones, each varying in width and density as shown in Fig.1.

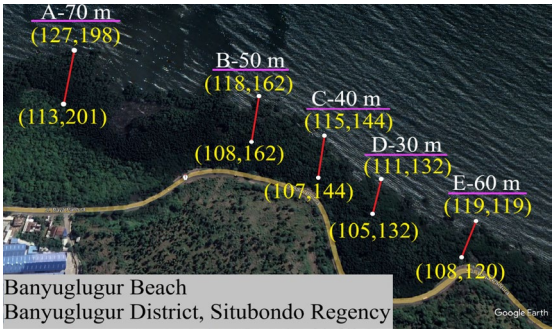

Fig.1 Research Sites

Zone A has a mangrove forest width of 70 m, Zone B has a width of 50 m, Zone C has a width of 40 m, Zone D has a width of 30 m, and Zone E has a mangrove forest width of 60 m.

3.2 Data Collection

The wind data were collected from the Meteorology, Climatology, and Geophysics Agency (BMKG) station in Kalianget, Sumenep, over a period of 10 years. The bathymetric data were obtained from the National Bathymetric Data (BATNAS) with a resolution of 6 arc-seconds (185.22 meters) obtained from the Geospatial Information Agency. The tidal data were sourced from Geospatial Information Agency (BIG) with coordinates specific to the research location. The tidal duration in this modeling was used for 49 hours (January 27, 2021 at 00:00 to January 29, 2021 at 00:00).

The collection of tidal and wind data is adjusted according to its inherently limited availability. Wind data is abundant, as it is observed by the Meteorology, Climatology, and Geophysics Agency. In contrast to tidal data, field observations

are rarely conducted. However, a small amount of tidal height data is already sufficient, as tides can be accurately predicted due to the movement of the moon, earth, and sun, which consistently follow their orbits.

3.3 Research Methods

Wind is one of the dominant components in wave formation [21]. With an increase in the speed and duration of wind gusts, wave height will also be higher, especially in offshore area [22]. The increase in wind speed will result in higher energy transfer and higher waves during typically calmer seasons, leading to an enhanced correlation between wind energy and wave energy [23]. Wind speed information is acquired through direct measurements either above the sea level or on nearby land in proximity to the forecasted wave location [24]. In hindcasting, the wind data used is the wind speed measured at a height of 10 meters above the ground. In cases where wind speed is not measured at this height, an adjustment for height needs to be calculated [25].

Before wave forecasting is conducted, wind data is corrected, including corrections for height differences, location effects, and conversion into wind stress factors. Following this, effective fetch calculations are carried out [26] and wave hindcasting is performed using the Shore Protection Manual method. The wave height values obtained from hindcasting are used for modeling with Delft3D-Flow and Delft3D-Wave. In Delft3D-Flow, the input data consists of tidal data, while Delft3D-Wave uses processed wind data as input.

4. RESULTS AND DISCUSSION

4.1 Wind Data Processing

Wind data were obtained from the BMKG (Meteorology, Climatology, and Geophysics Agency) station in Kalianget, Sumenep Regency, for a period of 10 years, from September 2011 to August 2021. The wind data from BMKG Sumenep Regency were recorded at a height of 3 meters above ground level. The wind directions analyzed in this study are in total of 8 directions. These directions consist of north, northeast, east, southeast, south, southwest, west, and northwest.

The wind speed classification used ranges from 1 m/s to 21 m/s. The purpose of classifying wind directions is to determine the dominant wind direction from the 10-year data obtained for calculating wind data, which will be used as input data for the Delft3D program. To facilitate information retrieval, wind speed data in is transformed into a Wind Rose diagram (Fig. 2) to identify the dominant wind directions.

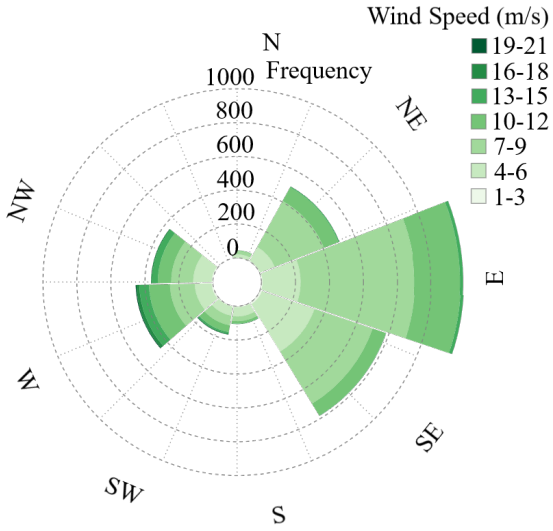

Fig.2 Windrose

The petals on a Wind Rose radiate outward from the center of the circle, representing the frequency or percentage of time the wind originates from a specific direction. The dominant wind direction is from the east, as shown in Fig.2, with a maximum speed of 16 m/s.

4.2 Hydrodynamic Modeling

The hydrodynamic simulation in this research utilizes a coupling model, namely Delft3D-Flow and Delft3D-Wave. Delft3D-Flow is a simulation program for multidimensional hydrodynamics that computes unsteady flow and transport phenomena arising from tidal and meteorological forces on a gridded system with established boundaries [27]. Delft3D-Flow is utilized for tidal simulation. Meanwhile, Delft3D-Wave computes wave propagation, wind-induced wave generation, non-linear wave-wave interaction, and dissipation across varying depths (deep, medium, and shallow waters) considering factors such as bottom topography, wind field, water surface, and current field [28]. As in this model, it requires input data of processed wind, including Significant Wave Height, Peak Period (Tp), and the most prevalent wind speed and direction.

4.2.1 Grid and Bathymetry

The grid shown in Fig.3 is created using the RGFGRID menu, with the smallest grid size having a resolution of 3x3 m and the largest grid having a resolution of 15x15 m, while the grid in the coastal area has a resolution of 4x4 m. The depth data in the model utilizes bathymetric data from BATNAS with a six-arcsecond resolution (approximately 180 meters), acquired from the Geospatial Information Agency and interpolated for each grid cell.

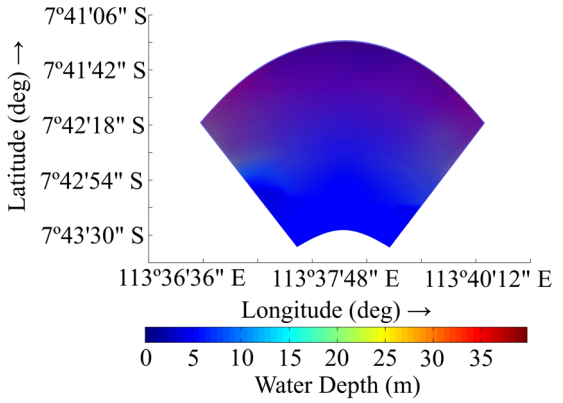

Fig.3 Grid and Bathymetry

Bathymetry data refers to information about underwater topography defined as the depth from bottom to the zero value [29]. It provides a detailed representation of the submerged terrain, including the depth of water at different locations [30]. To adjust the size of the bathymetric data to fit the research location, the bathymetry needs to be cut according to the requirements of the study. Resizing the bathymetry involves recording coordinate points on all four sides. Recording this coordinate point serves as a boundary for cutting bathymetry using QGIS for the research area [31].

4.2.2 Delft3D-Flow Input

The parameters to be inputted into Delft3D-Flow are grid data (grd) and bathymetry (dep) that have been interpolated based on the area domain. The time frame is set to limit the simulation start and end, from January 27, 2021, at 00:00 to January 29, 2021, at 00:00 WIB.

The processes involve selecting the parameters to be modeled. The boundaries are used to determine the model limits and also serve as the input location for tidal data. Physical parameters consist of columns for gravity, water density, constants, and viscosity values.

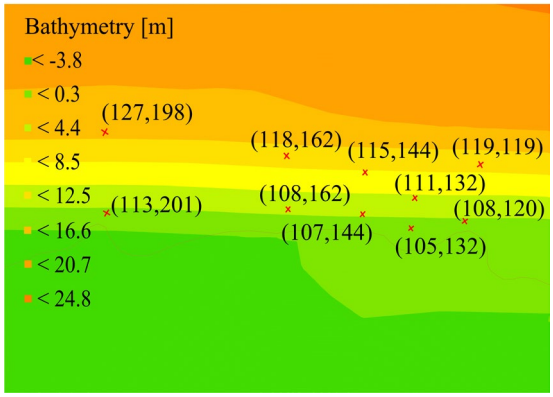

Fig.4 Observation Points

Monitoring involves the input of observation points to be reviewed, where the observation sub data is used to monitor the modeling of the selected area. In the modeling, ten observation points are placed in five zones. In each zone, two observation points are placed in front and behind the mangrove forest (Fig.4). The output menu is then used to configure the display of simulation results.

4.2.3 Creation of Mangrove Forests

The Mangrove Forest in this model is created using the Thin Dams menu within Delft3D-Flow. These thin dams are very thin objects defined at velocity points that prohibit flow exchange between two adjacent computational cells without reducing the total wetted surface and volume of the model [32]. The construction of thin dams in the model follows the grid shape and can be arranged both vertically and horizontally according to research needs. In this study, the thin dams used are arranged horizontally. The layout of mangrove forests with their widths and densities at each observation point is displayed in Fig.5.

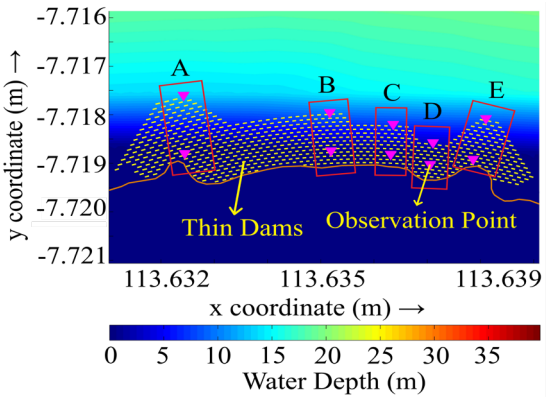

Fig.5 Mangrove Forest Layouts

The widths and densities of mangroves based on Fig.5 show that in Zone A it is 70 m, in Zone B it is 50 m, in Zone C it is 40 m, in Zone D it is 30 m, and in Zone E it is 60 m.

4.2.4 Delft3D-Wave Input

The parameters to be input into Delft3D-Wave include the grid and bathymetry, which must match those input into Delf3D-Flow. After that, the hydrodynamics section is filled in according to the model file that has been created. In the input boundaries section, values are entered based on the calculated significant wave height (Hs) of 3.8 m, peak period (Tp) of 7.7 seconds, and wind direction from the east as per the windrose diagram (Fig.2). The simulation time must be ensured to be the same with Delft3D-Flow starting from the date, hour, and minute to avoid failure in the simulation process.

4.3 Delft3D Modeling Result

The simulation results from Delft3D can be viewed using the QUICKPLOT menu, both for the outputs from the Delft3D-Flow model and the Delft3D-Wave model. The simulation output consists of visualizations of the model in the form of images and graphs displayed according to the specified date and time. These visualizations are also equipped with legend information, time, and the examined parameters. The simulation results from January 27, 2021, at 00:00 to January 29, 2021, at 00:00 WIB showed that the highest water level occurred on January 28, 2021, at 18:00 WIB.

The simulation results from all specified zones can be seen in Table 1. The table shows that the water level in the front and back of the mangrove in each zone is the same, measuring 1.04 m. This is because the five observation points are close to each other and are still within the same region, namely Banyuglugur Beach, so the coastal morphology conditions in these five zones are still similar. The wave period is closely related to the wavelength and wave propagation speed. The greater the wave period, the greater the wavelength [33]. Referring to Table 1, the wave period values for all zones in front of the mangrove are lower compared to those behind the mangrove. For example, the period in Zone A in front of the mangrove and behind it are 4.85 seconds, while behind the mangrove, it is 6.53 seconds. Conversely, the wavelength in front of the mangrove in Zone A is 36.27 meters, while behind the mangrove, it is 24.90 meters.

Table 1 Calculation Results for All Zones

Parameters	Zone A (70 m)		Zone B (50 m)		Zone C (40 m)		Zone D (30 m)		Zone E (60 m)	
	Front	Back	Front	Back	Front	Back	Front	Back	Front	Back
Water Level (m)	1.04	1.04	1.04	1.04	1.04	1.04	1.04	1.04	1.04	1.04
Wave Period (s)	4.85	6.53	5.08	6.98	5.17	6.90	5.58	7.14	5.26	7.39
Wave Length (m)	36.27	24.90	38.30	28.10	37.27	29.29	39.79	29.41	40.04	27.81
Wave Height (m)	1.73	0.86	1.82	1.12	1.82	1.19	1.73	1.26	1.92	1.06
Wave Propagation Velocity (m/s)	7.47	3.82	7.53	4.02	7.22	4.25	7.14	4.12	1.92	1.06
Wave Energy (J)	77036.7	26111.8	85302.3	38517.9	83194.7	42576.6	84199.2	45437.1	93998.1	36083.4
Wave Height Reduction (m)	0.88		0.70		0.64		0.47		0.86	
Wave Energy Reflection (J)	3056.17		2184.02		1553.72		1482.09		3211.05	
Dissipation Wave (J)	47868.72		44600.39		39064.39		37280.03		54703.66	
Wave Height Reduction (%)	50.63		38.45		34.87		26.99		44.73	
Dissipation Wave (%)	62.14		52.29		46.96		44.28		58.20	

The wave period is inversely proportional to the wave propagation speed. That is, the larger the wave period, which is the time it takes for a wave to pass a point, the smaller the wave propagation speed. Conversely, the smaller the wave period, the greater the speed of propagation. For example, the wave period in Zone A is 4.86 seconds in front of the mangrove and 6.53 seconds behind the mangrove. This value is inversely proportional to the wave propagation speed in the same zone, which is 7.47 m/s in front of the mangrove and 3.82 m/s behind the mangrove.

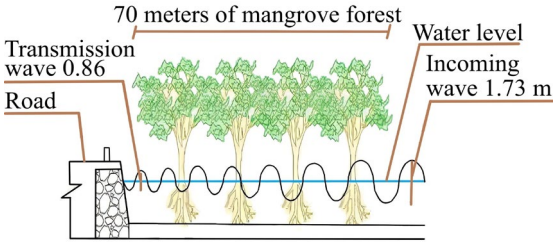

Fig.6 Illustration at Zone A

Fig. 6 illustrates Zone A. The incoming wave height that hits the front of the mangrove is 1.73 m. The wave moves through the mangrove forest, which has a width of 70 m. As per the characteristics of mangrove trees, they have effective aerial roots in reducing waves. However, the effectiveness of this vegetation in wave reduction is influenced by several factors such as tree density, mangrove thickness, tidal variations, and the effects of climate change on the mangrove ecosystem [34,35].

When the tidal wave moves through a dense forest consisting of tree trunks, aerial roots, and other vegetation, the flow velocity of water and wave energy will be impeded [36]. This mangrove will dampen waves in shallow waters faster than in deeper ones. In deeper waters, waves can pass through aerial roots, but lower branches can perform the same function [37]. Consequently, the transmitted wave in Fig.6 behind the mangrove forest becomes 0.86 m with a reduction in wave height of 0.88 m.

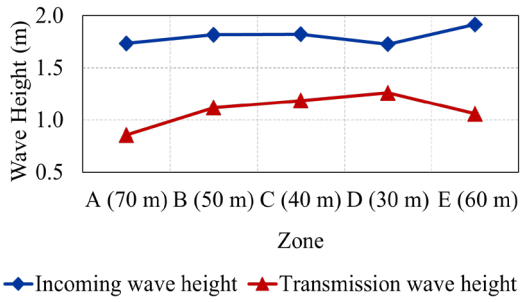

Fig.7 Comparison Chart of Wave Height

The difference in wave values between incoming waves and transmitted waves also applies to other zones, as shown in the graph in Fig.7. In Zone B, the initial wave of 1.82 m becomes 1.12 m with a reduction in wave height of 0.70, while in Zone C, the initial wave of 1.82 m becomes 1.19 m with a reduction in wave height of 0.64 m. Zones D and E have initial waves of 1.73 m and 1.92 m, which then become 1.26 m and 1.06 m, respectively. Consequently, these two zones experience a wave reduction of 0.47 m and 0.86 m.

Wave heights <1 m are categorized as a low threat index for mangrove vegetation, ranging from 1 to 2.5 m is categorized as a moderate threat, and >2.5 meters is categorized as a high threat index [38]. This indicates that the threat of mangrove forest damage at Banyuglugur Beach falls within the moderate index. These mangrove forests are still able to dampen waves but also potentially experience a decrease in function due to continuous wave impacts.

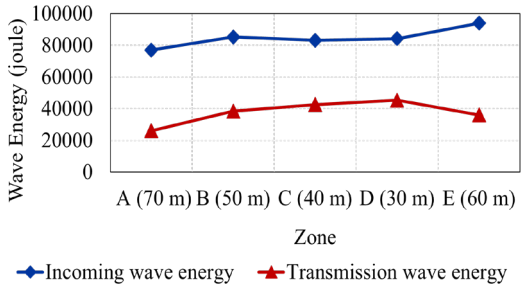

Fig.8 Comparison Chart of Wave Energy

The wave energy in Fig.8 with the highest value is located in front of the mangrove, specifically in Zone D, with an energy level of 93998.1 joules, while the lowest energy value is found in Zone A with an energy of 26111.8 joules. The magnitude of wave energy is directly proportional to its amplitude [39]. This means that waves with larger amplitudes carry more wave energy. Therefore, in this case, Zone D has the highest wave height or amplitude in front of the mangrove, with a value of 1.92 m, while Zone A has the smallest amplitude behind the mangrove, with a height of 0.86 m.

The magnitude of wave reflection energy is highest in Zone E, with a value of 3211.05 joules, while the lowest value is in Zone C, with an energy of 1553.72 joules. The reduction in wave height in Zone A is the highest, with a value of 0.88 compared to other zones. The amount of wave dissipation is influenced by the characteristics of the mangrove forest growing in each zone, as Zone E has the highest wave dissipation value, with an energy of 54703.66 joules.

The presence of mangrove forests on Banyuglugur Beach, based on simulation results, can contribute to coastal protection by safeguarding everything behind them. This nature-based coastal protector indicates that the waves experience an average wave height reduction of 0.71 meters. The highest wave height reduction is in Zone A, with a percentage of 50.63%, where the mangrove forest, which has a width and high density of 70 meters, can dampen wave energy by 62.14%. This indicates that the reduction in wave height within the mangrove forest depends on the width and density of the mangrove forest on the coastline.

5. CONCLUSIONS

A numerical simulation of the mangrove as a wave breaker on Banyuglugur Beach, Situbondo Regency, was conducted to assess its effectiveness against tides and wind dring the highest tide event. Mangroves with a density and width of 70 m in Zone A can reduce 62.14% of wave energy, while mangroves with a width of 50 m in Zone B can reduce 52.29% of wave energy. Zone C, with mangroves having a width of 40 m, can reduce 46.96% of wave energy. Mangroves in Zone D with a width of 30 m can reduce 44.28% of wave energy, and mangroves with a width of 60 m in Zone E can reduce 58.20% of wave energy.

The reduction in wave height within the mangrove forest depends on the width and density of the forest, and the morphology of mangrove trees relative to water depth, topography, and wave height. Waves reduce their speed optimally when passing through denser obstacles. Conversely, if the obstacles are less dense, the ability to reduce the waves will also decrease.

6. ACKNOWLEDGMENTS

The author would like to acknowledge the internal research grant from the Keris-Dimas Research Institute of the University of Jember in the fiscal year 2022, contract number 4226/UN25.3.1/LT/2022, which provided funding for this research.

7. REFERENCES

[1] Asari, N., Suratman, M. N., Ayob, N. A. M., and Hamid, N. H. A., Mangrove as a Natural Barrier to Environmental Risks and Coastal Protection, Mangroves: Ecology, Biodiversity and Management, 2021, pp. 305–322.

[2] Gijsman, R., Horstman, E. M., van der Wal, D., Friess, D. A., Swales, A., and Wijnberg, K. M., Nature-Based Engineering: A Review on Reducing Coastal Flood Risk With Mangroves, Frontiers in Marine Science, Vol. 8, Issue July, 2021, p. 702412.

[3] Cahyaningsih, Agustina Putri Deanova, Avyda Koza Pristiawati, Celin Maylani Ulumuddin, Yaya Ihya Kusumawati, Lia Setyawan, A. D., Causes and Impacts of Anthropogenic Activities on Mangrove Deforestation and Degradation in Indonesia, International Journal of Bonorowo Wetlands, Vol. 12, Issue 1, 2022, pp. 12–22.

[4] Wardhani, M. K., Rosyid, D. M., and Armono, H. D., Land Use Change of Mangrove Forest for Eco-Tourism in the South Coastal, Bangkalan, East Java-Indonesia, International Journal of GEOMATE, Vol. 23, Issue 98, 2022, pp. 136–146.

[5] Budiarti, A. W., Wijaya, N. I., and Bintoro, R. S., Land Suitability for Mangrove Ecotourism in Situbondo Regency, in Seminakel Proceeding, 2019, pp. 58–67.

[6] Romadhona, S., Mutmainnah, L., and Setiawati, T. C., Mangrove Seedling Cultivation and Revitalization Practices to Develop Mangrove Ecotourism in the Coastal Area of Agel Village, Jangkar Sub-district, Situbondo, Community Empowerment, Vol. 5, Issue 2, 2020, pp. 58–63.

[7] Trimanto, Hapsari, L., Yulistyarini, T., Budiharta, S., Danarto, S. A., Mas'udah, S., Damaiyani, J., Laksono, R. A., Lavianti, N., and Yunanto, B., Vegetation Diversity and Stand Carbon Stocks in Wana Wisata Tampora, Situbondo, East Java, Wallacea Journal of Forestry Research, Vol. 10, Issue 2, 2021, pp. 103–116.

[8] Environmental Agency, Performance Report of The Environmental Agency 2021, 2022, pp. 1–179.

[9] Muliati, Y., Tawekal, R. L., Wurjanto, A., Kelvin, J., and Pranowo, W. S., Wind Wave Modeling in Natuna Sea: A Comparison Among Swan, Seafine, and Era-Interim, International Journal of GEOMATE, Vol. 16, Issue 54, 2019, pp. 176–184.

[10] Tan, I. T. S., Hassan, N. M. K. N., and Teh, H. M., Assessment of Wave Attenuation Performance of The Tanjung Piai Breakwater Using Spectral Wave Analysis, International Journal of Integrated Engineering, Vol. 15, Issue 1, 2023, pp. 286–298.

[11] Abdul Azeez, S., Gnanappazham, L., Muraleedharan, K. R., Revichandran, C., John, S., Seena, G., and Thomas, J., Multi-Decadal Changes of Mangrove Forest and Its Response to The Tidal Dynamics of Thane Creek, Mumbai, Journal of Sea Research, Vol. 180, 2022, p. 102162.

[12] Lee, W. K., Tay, S. H. X., Ooi, S. K., and Friess, D. A., Potential Short Wave Attenuation Function of Disturbed Mangroves, Estuarine, Coastal and Shelf Science, Vol. 248, 2021, p. 106747.

[13] Tarya, A., Sunaringati, L. C., and Ningsih, N. S., Mangrove Density Impacts on Tidal Dynamic in Segara Anakan Lagoon, Indonesia, in Journal of Physics: Conference Series, IOP Publishing, 2019, p. 012060.

[14] Xie, D., Schwarz, C., Kleinhans, M. G., Zhou, Z., and van Maanen, B., Implications of Coastal Conditions and Sea-Level Rise on Mangrove Vulnerability: A Bio-Morphodynamic Modeling Study, Journal of Geophysical Research: Earth Surface, Vol. 127, Issue 3, 2022, pp. 1–28.

[15] Fauzah, S., Tarya, A., and Ningsih, N. S., Three-Dimensional Numerical Modelling of Tidal Current in Balikpapan Bay Using Delft 3D, in IOP Conference Series: Earth and Environmental Science, IOP Publishing, 2021, p. 012051.

[16] Deltares, 3D/2D Modelling Suite For Integral Water Solutions: RFGRID, 2023, pp. 1–145.

[17] Fringer, O. B., Dawson, C. N., He, R., Ralston, D. K., and Zhang, Y. J., The Future of Coastal and Estuarine Modeling: Findings from a Workshop, Ocean Modelling, Vol. 143, 2019, p. 101458.

[18] Damarnegara, S., Ali, R. P., and Ansori, M. B., Transcritical Flow Simulation Using Shallow Water Equation Model, Journal of Civil Engineering, Vol. 34, Issue 2, 2019, pp. 55–60.

[19] Sofiana, R., Wiyono, R. U. A., and Nurtjahjaningtyas, I., Tsunami Mitigation Strategy at Watu Ulo Beach Based on Numerical Modeling Using Delft3D-Flow, UKaRsT, Vol. 6, Issue 2, 2022, pp. 158–173.

[20] Cao, Z., Zhou, J., Liu, A., Sun, D., Yu, B., and

Wei, J., A Three Dimensional Coupled VOF and Level Set (VOSET) Method with and Without Phase Change on General Curvilinear Grids, Chemical Engineering Science, Vol. 223, 2020, p. 115705.
[21] Wiyono, R. U. A., Fadhilla, A., Ma, A. R. M., Halik, G., Widiarti, W. Y., and Hidayah, E., Effect of Breakwater Layout on Waves at Puger Beach Jember with Delft3D Modeling, in E3S Web of Conferences, ICST UGM, 2023, p. 01002.
[22] Joseph, C. and Latupeirissa, E. O., Analysis of Coastal Line Changes and Planning of Coastal Protection Structures in Negeri Amdua, Amahai District, Central Maluku Regency, Journal of Manumata, Vol. 8, Issue 2, 2022, pp. 152–166.
[23] Lira-Loarca, A., Ferrari, F., Mazzino, A., and Besio, G., Future Wind and Wave Energy Resources and Exploitability in The Mediterranean Sea By 2100, Applied Energy, Vol. 302, 2021, p. 117492.
[24] Pratiwi, D., Time Series Hydro-Oceanographic Study for Long Port Development, Journal of Infrastructural in Civil Engineering, Vol. 1, Issue 01, 2020, pp. 1–13.
[25] Triatmodjo, B., Beach Engineering. Beta Offset, 1999, pp. 1–405.
[26] Triatmodjo, B., Coastal Building Planning. Beta Offset, 2006, pp. 1–327.
[27] Deltares, 3D/2D Modelling Suite For Integral Water Solutions: Functional Description, 2024, pp. 1–47.
[28] Deltares, 3D/2D Modelling Suite For Integral Water Solutions: Wave, 2024, pp. 1–219.
[29] Erena, M., Domínguez, J. A., Atenza, J. F., García-Galiano, S., Soria, J., and Pérez-Ruzafa, Á., Bathymetry Time Series Using High Spatial Resolution Satellite Images, Water, Vol. 12, Issue 2, 2020, p. 531.
[30] Li, Z., Peng, Z., Zhang, Z., Chu, Y., Xu, C., Yao, S., García-Fernández, Á. F., Zhu, X., Yue, Y., Levers, A., Zhang, J., and Ma, J., Exploring Modern Bathymetry: A Comprehensive Review of Data Acquisition Devices, Model Accuracy, and Interpolation Techniques for Enhanced Underwater Mapping, Frontiers in Marine Science, Vol. 10, 2023, p. 1178845.
[31] Lemenkova, P., An Empirical Study of R Applications for Data Analysis in Marine Geology, Marine Science and Technology Bulletin, Vol. 8, Issue 1, 2019, pp. 1–9.
[32] Deltares, 3D/2D Modelling Suite For Integral Water Solutions: Hydro-Morphodynamics, 2023, pp. 1–747.
[33] Nastain, Suripin, Yuwono, N., and Sriyana, I., Wave Diffraction Through Low-Threshold Half Cylinder Breakwater, Scientific Journal of Design and Construction, Vol. 20, Issue 2, 2021, pp. 118–128.
[34] Dwipa Kusuma Maharani, M., Masyitha Amelia, J., and Sari Br Sitepu, G., Ecosystem Management of Mangroves as Disaster Mitigation Efforts in the Province of Aceh, Journal of Biological Education at Undiksha, Vol. 9, Issue 2, 2022, pp. 150–158.
[35] Roy, P., Pal, S. C., Chakrabortty, R., Chowdhuri, I., Saha, A., and Shit, M., Effects of Climate Change and Sea-Level Rise on Coastal Habitat: Vulnerability Assessment, Adaptation Strategies and Policy Recommendations, Journal of Environmental Management, Vol. 330, 2023, p. 117187.
[36] Dasgupta, S., Islam, M. S., Huq, M., Khan, Z. H., and Hasib, M. R., Quantifying The Protective Capacity of Mangroves from Storm Surges in Coastal Bangladesh, PLoS ONE, Vol. 14, Issue 3, 2019, p. e0214079.
[37] McIvor, A., Möller, I., and Spencer, T., Reduction of Wind and Swell Waves By Mangroves, 2012, pp. 1–127.
[38] Head of the National Disaster Management Agency Regulation Number 02 of 2012 Regarding General Guidelines for Disaster Risk Assessment, National Disaster Management Agency, 2012, pp. 1–62.
[39] Elisa, M. S. and Herliana, F., The concept of Waves & Their Applications in Life. Syiah Kuala University Press, 2023, pp. 1–140.